

Effect of hot-carrier energy relaxation on main properties of collapsing field domains in avalanching GaAs

V. Palankovski, S. Vainshtein, V. Yuferev, J. Kostamovaara, and V. Egorkin

Citation: [Applied Physics Letters](#) **106**, 183505 (2015); doi: 10.1063/1.4921006

View online: <http://dx.doi.org/10.1063/1.4921006>

View Table of Contents: <http://scitation.aip.org/content/aip/journal/apl/106/18?ver=pdfcov>

Published by the [AIP Publishing](#)

Articles you may be interested in

[Ultrafast spectroscopy of impact ionization and avalanche multiplication in GaAs](#)

Appl. Phys. Lett. **88**, 132113 (2006); 10.1063/1.2191880

[Magnetic-field-controllable avalanche breakdown and giant magnetoresistive effects in Gold/semi-insulating-GaAs Schottky diode](#)

Appl. Phys. Lett. **85**, 5643 (2004); 10.1063/1.1834733

[Electric-field-induced reversible avalanche breakdown in a GaAs microcrystal due to cross band gap impact ionization](#)

Appl. Phys. Lett. **83**, 704 (2003); 10.1063/1.1595712

[Full band Monte Carlo modeling of impact ionization, avalanche multiplication, and noise in submicron GaAs p + -i-n + diodes](#)

J. Appl. Phys. **87**, 7885 (2000); 10.1063/1.373472

[Hot electron transport in n -GaAs field emitter at nitrogen temperature](#)

J. Appl. Phys. **82**, 670 (1997); 10.1063/1.365597

A promotional banner for Applied Physics Reviews. On the left is a thumbnail image of the journal cover for 'Applied Physics Reviews', which shows a diagram of a device structure. The main part of the banner has a blue background with a molecular model of a crystal lattice. The text 'NEW Special Topic Sections' is prominently displayed in white. Below this, on an orange background, it says 'NOW ONLINE' in yellow, followed by 'Lithium Niobate Properties and Applications: Reviews of Emerging Trends' in white. The AIP Applied Physics Reviews logo is in the bottom right corner.

Effect of hot-carrier energy relaxation on main properties of collapsing field domains in avalanching GaAs

V. Palankovski,^{1,2,a)} S. Vainshtein,² V. Yuferev,³ J. Kostamovaara,² and V. Egorkin⁴

¹Institute for Microelectronics, Technical University Vienna, 1040 Vienna, Austria

²Electronics Laboratory, Department of Electrical Engineering, University of Oulu, 90014 Oulu, Finland

³Department of Applied Mathematics and Mathematical Physics, Ioffe Institute, 194021 St. Petersburg, Russia

⁴National Research University of Electronic Technology MIET, 124498 Zelenograd, Moscow, Russia

(Received 3 December 2014; accepted 30 April 2015; published online 7 May 2015)

Multiple “collapsing” field domains are a physical reason for superfast switching and sub-terahertz (sub-THz) emission experimentally observed in powerfully avalanching GaAs structures. This phenomenon, however, has been studied so far without considering carrier energy relaxation and that essentially has restricted the possibility of correct interpretation of experimental results. Here, we apply a hydrodynamic approach accounting for non-local hot-carrier effects. The results confirm the collapsing domain concept, but show that the domains cannot reduce well below 100 nm in width, since a moving collapsing domain leaves behind it a tail of hot carriers, which causes broadening in the rear wall of the domain. This puts principal restrictions on the emission band achievable with our unique avalanche mm-wave source to about 1 THz. Another finding suggested here is a physical mechanism for the single collapsing domain’s quasi-steady-state motion determined by powerful impact ionization. The results are of significance for physical interpretation of properties of our pulsed sub-THz source, which has recently demonstrated its application potential in mm-wave imaging in both amplitude and time-domain pulse modes with picosecond time-of-flight precision. © 2015 AIP Publishing LLC. [<http://dx.doi.org/10.1063/1.4921006>]

A phenomenon of practically instantaneous formation of dense electron-hole plasma in a GaAs bipolar transistor structure during its superfast switching (see Fig. 1(a)) has been shown to be caused by a train of powerfully avalanching electric field domains,¹ which determine also the operation of other avalanche devices, e.g., photoconductive semiconductor switches (PCSS).² The domains appear (see Fig. 1(b)) and locally split the dense electron-hole (e-h) plasma formed at earlier stages of avalanche switching. As the domains move towards the n^+ sub-collector with a velocity of ~ 100 nm/ps, powerful impact ionization in them increases the plasma density, while the last one causes domain shrinkage and growth in their amplitude and consequently also in the ionization rate.³ The extremely high amplitude (~ 0.5 – 0.6 MV/cm) and nanometer-scale width achieved by these domains during the transient are determined by negative differential mobility (NDM) at electric fields exceeding the impact ionization threshold⁴ (see the inset of Fig. 1). These domains have been termed “collapsing,”⁵ because they shrink drastically during the switching transient and finally disappear as soon as the powerful impact ionization in the domains elevates the carrier density above $\sim 10^{19}$ cm⁻³.

Emitters, based on the classical Gunn effect,⁶ have frequency limitations, which are softened in the so-called bipolar Gunn effect (predicted theoretically,⁷ confirmed numerically,⁵ but never proved experimentally). The collapsing field domains allow for even higher frequencies to be reached. Furthermore, a fundamental limitation for maximum generated sub-THz power exists not only for

“standard” Gunn oscillators but also for a large variety of well-established and optimized solid-state devices (IMPact ionization Avalanche Transit-Time, TUNNELing Transit-Time, Resonant-Tunneling Diodes,⁸ superlattices,⁹ plasma

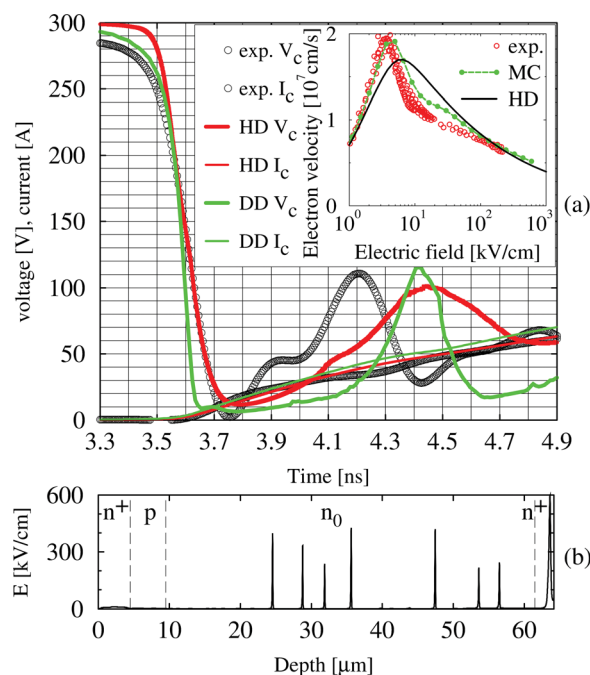


FIG. 1. (a) Collector voltage and collector current temporal profiles measured during superfast avalanche switching of a bipolar GaAs transistor, and simulated in this work using DD and HD models and (b) electric field profile along the switching channel in the HD model at 3.58 ns. Ultra-narrow, ultra-high-amplitude (“collapsing”) domains are caused by NDM at ultra-high fields (inset). Experimental (exp.) and MC data, shown in the inset, are from Ref. 3 and references therein.

^{a)}Electronic mail: palankovski@iue.tuwien.ac.at

wave electronics (meaning interface waves in n-channels of FETs),¹⁰ linear-mode RF transistors,¹¹ etc.). This is the trade-off between using larger area for increasing the power and the resulting larger capacitance of the structure which shunts the signal. Unlike those devices, our simple miniature emitter, despite of its infancy, already provides ps-range pulses of huge power density (e.g., 1–10 MW/cm² at 130 GHz) at room temperature, which allowed to demonstrate mm-wave imaging in both amplitude and time-domain pulse modes with picosecond time-of-flight precision.¹²

Good agreement between measured voltage waveforms during superfast avalanche switching and drift-diffusion (DD) modeling¹³ introduced the collapsing domain concept, however, validate moderate carrier plasma densities. At higher densities, the carrier energy relaxation has to be taken into account, because the domain width W_D becomes comparable to $v_c \times \tau_c$, where v_c is the carrier velocity and τ_c is the energy relaxation time. Assuming $v_c \sim 10^7$ cm/s and $\tau_c \sim 0.2$ – 0.5 ps (see below), domains of $W_D < 50$ nm should not be analyzed using the DD transport model. Thus, accounting for hot-carrier effects is critically important, especially for studying powerful terahertz emission, which corresponds to $W_D \sim 10$ – 100 nm (in DD modeling) when the e-h plasma density exceeds $\sim 10^{18}$ cm⁻³ (which is the case in our emitters). Here, we use hydrodynamic (HD) modeling to overcome this limitation in the DD approach. The HD simulation results confirm the collapsing domain concept, in general, and show much better agreement with measured voltage and current waveforms in GaAs avalanche transistors^{1,3,11} up to high carrier densities. Demonstrated and physically interpreted saturation of W_D is of major importance for future application of the developed tool for analysis of the experimental results obtained for unique sub-THz emitters. (Those emitters have proven their high application potential,¹² but their structure and operation principles have not been published so far because of lacking appropriate modeling.) This approach is suited also for analysis of other GaAs-based avalanche switches such as PCSS.² Also, a qualitative interpretation is given in this paper for the main physical mechanisms responsible for the formation and motion of collapsing domains, which have so far been investigated only numerically.

The dynamics and evolution of ionizing multiple domains in the conducting channel are considered. These appear in the n-collector of a GaAs bipolar transistor during its superfast avalanche switching and cause the current density to increase from ~ 10 kA/cm² to ~ 10 MA/cm² within as short a time as ~ 150 ps. The device structure, chip design, and experimental conditions¹³ are used as inputs for our one-dimensional DD and HD simulations of the switching channel. Unlike DD,^{1,3,13} HD approach has not been applied to the problem before. In the DD approach, the energy of carriers is completely determined by instantaneous local value of the electric field. In reality, when the electric field varies rapidly, the average carrier energy lags behind it and the mobility depends primarily on the average energy and not on the electric field.¹⁴ Similarly several other processes such as impact ionization are more accurately described by an energy model, because they depend on the distribution function rather than on the electric field itself.^{15,16} Since the pioneering work of Stratton¹⁷ and Bløtkejaer,¹⁸ various transport

models have been proposed, which account for the average carrier energy or temperature (see, e.g., Refs. 19–25). In this work, the HD transport model adopted in Minimos-NT is used. This is a four-moment energy transport model,¹⁴ which provides the best physics-based description of the problem at reasonable computational cost. Compared with the DD model, the HD model is extended by means of additional balance equations for the average carrier energies, and in this approach the mobility, diffusion coefficients, and impact ionization coefficients are functions of the carrier temperature.

The high-field hole mobility is modeled after Hänsch^{26,27}

$$\mu_p = \frac{\mu_p^L}{1 + \alpha_p},$$

where

$$\alpha_p = \frac{3k_B\mu_p^L(T_p - T_L)}{2q\tau_{e,p}(\nu_{p,sat})^2}. \quad (1)$$

For electrons (1) was modified to account for NDM effects²⁸

$$\mu_n = \frac{\mu_n^L}{(1 + \alpha_n^4)^{0.25}} \frac{T_L}{T_n},$$

where

$$\alpha_n = \frac{3k_B\mu_n^L(T_n - T_L)}{2q\tau_{e,n}(\nu_f)^2}. \quad (2)$$

μ_p^L and μ_n^L are the low-field carrier mobilities, depending on the doping concentration, T_p , T_n and T_L are the carrier and lattice temperatures, respectively, $\tau_{e,p}$ and $\tau_{e,n}$ are the carrier energy and relaxation times, $\nu_{p,sat}$ is the hole saturation velocity, and ν_f is a parameter used together with the T_L/T_n term to model the steady velocity decrease at high fields.²⁸

Radiative recombination was taken into account by using a radiation constant 2×10^{-10} cm⁻³ s⁻¹. Other recombination mechanisms were ignored. The impact ionization coefficients have the form $\alpha_{n,p} = A_{n,p} \exp\left(-\frac{B_{n,p}E_g}{k_B T_{n,p}}\right)$, where E_g is the GaAs bandgap energy, $A_n = 10^{15}$ s⁻¹, $A_p = 5 \times 10^{14}$ s⁻¹, and $B_{n,p} = 4$, based on Monte Carlo (MC) data.²⁹

Constant energy relaxation times $\tau_{e,n} = 0.5$ ps and $\tau_{e,p} = 0.25$ ps were selected in agreement with the MC simulation results for electrons⁴ (0.4–0.5 ps) and for holes³⁰ (0.1–0.3 ps), and $\nu_f = 3 \times 10^7$ cm/s. This set of parameters not only provides best agreement with the experimental current and voltage temporal profiles (Fig. 1) but also reproduces the velocity-field characteristics obtained earlier experimentally and by MC simulations³ (inset of Fig. 1). All other material model parameters are kept as given in Ref. 31.

Comparison of HD and DD modeling results shows that the collapsing domain parameters show random fluctuations around certain values for each time instant and in different spatial positions, but a certain correlation exists between the average e-h plasma density along the channel (increasing during the transient) and the full-width-at-half-maximum (FWHM) of an individual domain.³ We used this correlation in Fig. 2 to

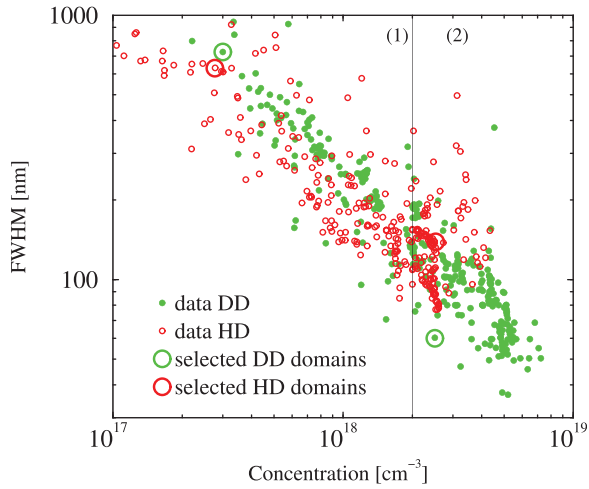


FIG. 2. Correlation between domain width W_D and e-h plasma density surrounding the domain in the channel during the switching simulated by two methods: DD and HD. The large hollow circles mark the positions of the DD and HD domains selected for detailed comparison (see Fig. 3) and the corresponding low and high plasma densities (at the beginning and end of the switching transient, respectively).

pinpoint similarities and differences between the DD and HD simulation results for the same structure under identical conditions. The dependence of the domain width W_D on the carrier density $n \approx p$ is similar up to an e-h plasma density of $\sim 2 \times 10^{18} \text{ cm}^{-3}$ ($W_D \approx 90\text{--}150 \text{ nm}$), but at higher concentrations (instants above $\sim 3.6 \text{ ns}$, see Fig. 1(a)) the difference becomes considerable. Namely, W_D drops to $30\text{--}40 \text{ nm}$ in some cases in DD simulations ($\sim 55 \text{ nm}$ on average), while it saturates at $\sim 100 \text{ nm}$ in HD modeling. This means that at similar domain amplitudes and similar number of domains in the channel the collector voltage should reduce slower in HD than in DD (see waveforms in Fig. 1(a)), and comparison with the experiment speaks in favor of the HD model as soon as it concerns the fast switching stage (interval $3.6\text{--}3.7 \text{ ns}$). Certain difference still exists between the measured and simulated voltage for $t > 3.75 \text{ ns}$, which we attribute to a faster reduction in the carrier density in the experiment than in the modeling due to (i) lateral spreading of the carriers out of the switching channel is not accounted in one-dimensional simulations and (ii) stimulated carrier recombination along the channel may cause higher carrier losses than only spontaneous recombination accounted in the simulations. Fig. 3 shows a comparison between the profiles of “typical” domains produced by DD and HD models near the beginning (a)–(c) and near the end (d)–(f) of the fast switching stage (the four domains selected for comparison are marked by circles in Fig. 2). Figs. 3(a)–3(c) compare similar “broad” DD and HD domains ($W_D \sim 700 \text{ nm}$ in both cases), so that we conclude that both models arrive at about the same result given moderate carrier densities. The electric field (a) and carrier density profiles (b) are shown for both DD and HD, while the carrier temperatures (c) are from HD simulations only. The nearly analogous profiles shown in (d)–(f) correspond to the “narrowest” domains for each model at a later transient instant and much higher than for (a)–(c) plasma densities. Here, for comparable between DD and HD carrier densities we find a significant difference in W_D , a fact of essential importance both for a physical understanding of the phenomenon and for its applications. Indeed, a highly

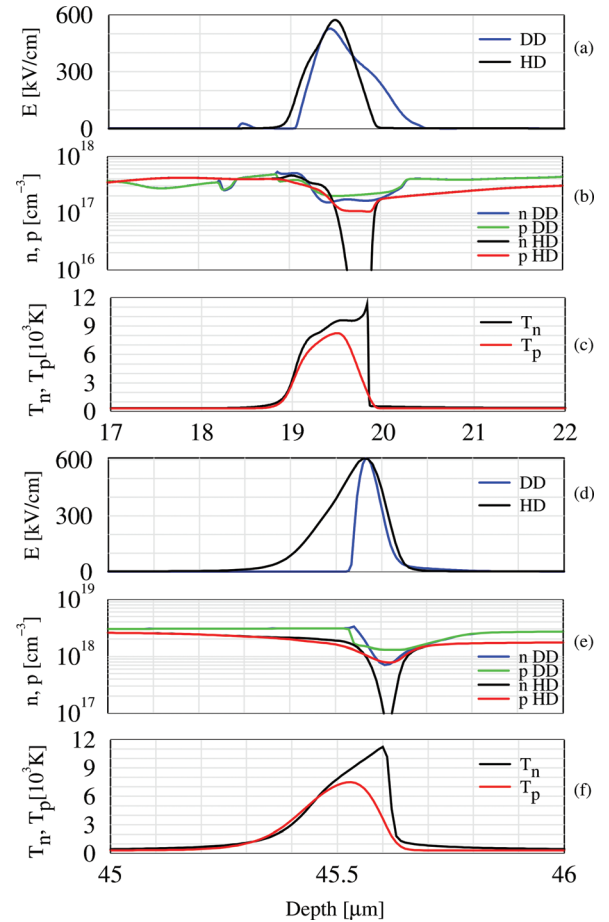


FIG. 3. Simulated spatial profiles of the electric field (a) and (d), electron and hole densities (b) and (e), and electron and hole temperatures (c) and (f) for a “broad” (a)–(c) and a “narrow” (d)–(f) domain. The DD and HD models used are labeled. The carrier temperatures (c) and (f) differ from the lattice temperature only in the HD approach. All four domains are selected at different instants, aiming at comparable e-h plasma densities (see corresponding circles in Fig. 2). The depth coordinate is shifted to match the peaks in the DD and HD domains. The domains move to the right.

challenging prospect for forthcoming mm-wave radars and active imaging could be a shifting of the emission spectrum from ~ 100 to 300 GHz towards $\sim 1 \text{ THz}$ or even higher. The minimal characteristic time for domain instabilities that determines the high-frequency boundary of the emission band should be comparable⁵ to the minimal W_D divided by the domain spread velocity $v_D \approx 10^7 \text{ cm/s} = 100 \text{ nm/ps}$. Physically, the minimal W_D is determined by delicate aspects of carrier transport in low-dimensional structures,¹⁵ where the electron velocity can vary from $\sim 10^8 \text{ cm/s}$ in a ballistic regime³² to $\sim 50 \text{ nm/ps}$ in a steady-state with extreme fields.⁴ The main focus for further discussions (and of this paper in general) will be on demonstrating and interpreting the lower limit which the HD model imposes on the domain width.

Powerful ionization in the collapsing domains results in fast and very significant growth in the e-h plasma density. This normally leads to monotonic temporal domain shrinkage due to the increased charge in the dipole on account of significant plasma splitting around a domain (see Figs. 3(b), 3(e), and DD). This tendency also manifests itself in HD modeling, but is violated at high carrier densities when W_D saturates at $\sim 100 \text{ nm}$ (see Fig. 2). (In a number of other simulations of collapsing domains for various structures, we

have not found any further significant reduction in the width of a *moving* domain at even higher plasma densities in the HD approach, despite the fact that DD modeling permits reduction of W_D to as low as ~ 10 nm). Before providing an interpretation of this main finding of our work, let us first explain the formation and motion of collapsing domains.

No analytical theory exists for collapsing field domains. These domains were introduced and described only through comparisons between physical and numerical experiments in Refs. 1, 3–5, and 13 and not even a qualitative physical understanding exists for this phenomenon that differs radically from a classical Gunn effect.

The DD rear domain wall: Let the narrow (~ 50 nm) DD domain move to the right (towards the n^+ sub-collector) with a velocity $v_D \approx v_0 = 100$ nm/ps,^{1,3} which is equal to the saturated hole velocity $v_{p,sat}$ (moving to the left) and practically twice as large as the electron velocity v_n within the high-field domain^{1,4} (see the inset of Fig. 1). The electrons forming the left (rear) domain wall are situated in a very high electric field (up to 600 kV/cm) and their velocity is certainly less than v_0 (see the inset of Fig. 1 and Refs. 1 and 4). This means that they can never reach the domain, and the domain motion is *not* associated with the electrons “attacking” the rear wall from the left. Arriving in the domain from the right are holes having a (saturated) velocity of $2v_0$ with respect to the domain and electrons which move in the same direction as the domain, but with a ~ 0.3 – $0.5v_0$ slower velocity. Thus, each electron captured by the front (right) wall of the domain from the e-h plasma spends a time in the domain that is longer than that spent by a hole by a factor of at least 4. Then the impact ionization, which is mainly determined by the electrons (arriving from the right or “born” inside the domain), will form a “new” negatively charged left wall, causing the rear wall of the domain to move to a new position to the right. It is important to note that there is no restriction on the sharpness of the rear wall of the domain in the DD model if we consider the requirement of total current J_{tot} conservation:

$$J_{tot} = (J_e^{drift} + J_e^{diff}) + (J_h^{drift} + J_h^{diff}) + J_{displ} = \text{const.} \quad (3)$$

Indeed, when the carriers leave the domain to the left and appear in a weak field, the large negative displacement current J_{displ} should be compensated for by a powerful increase in the conductivity current $(J_e^{drift} + J_e^{diff}) + (J_h^{drift} + J_h^{diff})$. This is realized in the DD model by means of a sharp increase in both the hole concentration (Fig. 3(e)) and the electron velocity (inset of Fig. 1).

In the discussion above, we essentially used an assumption that the domain velocity v_D is larger than the velocity v_n of the electrons moving inside the rear domain wall. This assumption is based on the fact that, considering all the simulations, the collapsing domains never move faster than $2v_0$ or slower than v_n . The latter observation can be easily understood, since if v_D were to decrease to the value of v_n , this would cause an unlimited accumulation of impact-generated electrons in the domain. This feature of the collapsing domains marks the principal difference with respect to the *classical* Gunn effect, in which the domain velocity is exactly equal to that of the electrons surrounding the domain.

The front domain wall in both the DD and HD approaches is mainly determined by charged holes (see Fig. 3(e)). In the DD model, $J_{displ} \sim dE/dt$ increases very significantly at the front of the domain, while $(J_h^{drift} + J_h^{diff})$ is not reduced since the reduction in the hole concentration p due to the increased drift velocity is compensated for by the diffusion flux J_h^{diff} . Thus, the increase in J_{displ} (see Eq. (3)) has to be compensated for by reductions in the electron currents $(J_e^{drift} + J_e^{diff})$, and a considerable part of this is associated with a reduction in the electron concentration to well below that of the holes. In HD modeling, the electron concentration profile is more sophisticated, but the result is the same: The electron density is significantly lower than that of the holes and the front domain wall, similar in both DD and HD approaches, is mainly determined by the hole density (i.e., by the carrier density in the e-h plasma before the front of the domain).

The HD left (rear) domain wall: The most important result obtained from the HD modeling is that saturation occurs in $W_D \sim 100$ nm so that any further increase in the carrier density in the switching channel will not cause domain shrinkage below this value. This is associated with the broadening in the left wall of the moving domain, see Figs. 3(d)–3(f), and a correlation between the field “tail” and that of the carrier temperature gives a hint as to the physical explanation for this effect. (In the next paragraph, it will be proven that the thermal tail causes broadening of the electric field distribution). Let us define τ_R as an effective time of carrier energy relaxation behind the domain moving with velocity v_D , then a characteristic size of the hot carriers’ (and the field domain W_{tail}) tail will be $W_{tail} = v_D \times \tau_R$. Given the characteristic tail size $W_{tail} \sim 100$ nm (comparable to W_D) and a characteristic domain velocity $v_D \approx v_0 = 10^7$ cm/s, we obtain an effective relaxation time $\tau_R \sim 1$ ps. This value is comparable but somewhat larger than the energy relaxation times for the electrons and holes τ_c , because in the domain tail the carrier heating continues at a reducing rate, however, which makes W_{tail} to be larger than $v_D \times \tau_c$.

The only point which requires explanation is why the rear wall of the domain expands to the same size as the hot carrier tail. Our explanation is again based on the total current conservation equation (3) and is obtained by way of contradictions. Let us assume that the rear wall of the domain is sharp, while the carrier temperatures at the same spatial point remain high. This would result in a sudden drop in the conductivity current due to reduced field, while the carrier mobilities remain low because of the high carrier temperatures. Total current conservation will then require a large displacement current density $J_{displ} \sim dE/dt$. This would mean temporal growth in the electric field, providing a broad field tail to the left comparable with that of the carrier temperature (Figs. 3(d) and 3(f)).

In conclusion, the hydrodynamic transport model, accounting for non-local hot-carrier effects, confirmed in general terms the concept of multiple ultra-narrow, ultra-high-amplitude, and powerfully avalanching (“collapsing”) field domains predicted earlier using the drift-diffusion approach. It is shown that hot-carrier effects prevent reduction of domain width below 50–100 nm. This finding is of essential importance when considering the terahertz emission

caused by the collapsing domains. A mechanism of the collapsing domains' motion is suggested, which strictly requires the domains to move faster than the electrons at extreme fields and cannot exist without powerful impact ionization.

The authors thank CMNT for engineering support, and TEKES, the Academy of Finland, and the Austrian Science Fund FWF for financial support.

- ¹S. Vainshtein, V. Yuferev, and J. Kostamovaara, "Ultra-high field multiple Gunn domains as the physical reason for superfast (picosecond range) switching of a bipolar GaAs transistor," *J. Appl. Phys.* **97**, 024502 (2005).
- ²L. Hu, J. Su, Z. Ding, Q. Hao, and X. Yuan, "Investigation on properties of ultrafast switching in a bulk gallium arsenide avalanche semiconductor switch," *J. Appl. Phys.* **115**, 094503 (2014).
- ³S. Vainshtein, V. Yuferev, and J. Kostamovaara, "Analyses of the picosecond range transient in a high-power switch based on a bipolar GaAs transistor structure," *IEEE Trans. Electron Devices* **52**, 2760 (2005).
- ⁴S. Vainshtein, V. Yuferev, V. Palankovski, D. S. Ong, and J. Kostamovaara, "Negative differential mobility in GaAs at ultra-high fields: Comparison between an experiment and simulations," *Appl. Phys. Lett.* **92**, 062114 (2008).
- ⁵S. Vainshtein, J. Kostamovaara, V. Yuferev, W. Knap, A. Fatimy, and N. Diakonova, "Terahertz emission from collapsing field domains during switching of a gallium arsenide bipolar transistor," *Phys. Rev. Lett.* **99**, 176601 (2007).
- ⁶J. B. Gunn, "Microwave oscillation of current in III-V semiconductors," *Solid State Commun.* **1**, 88 (1963).
- ⁷B. L. Gelmont and M. S. Shur, "High-field domains in Gunn diodes with two types of carriers," *Sov. Phys. JETP* **33**, 1234 (1971).
- ⁸H. Eisele and G. I. Haddad, "Two-terminal millimeter-wave sources," *IEEE Trans. Microwave Theory Tech.* **46**, 739 (1998).
- ⁹L. L. Bonilla and H. T. Grahn, "Non-linear dynamics of semiconductor superlattices," *Rep. Prog. Phys.* **68**, 577 (2005).
- ¹⁰M. Dyakonov and M. Shur, "Shallow water analogy for a ballistic field effect transistor: New mechanism of plasma wave generation by dc current," *Phys. Rev. Lett.* **71**, 2465 (1993).
- ¹¹M. Seo, M. Urteaga, J. Hacker, A. Young, Z. Griffith, V. Jain, R. Pierson, P. Rowell, A. Skalare, A. Peralta, R. Lin, D. Pukala, and M. Rodwell, "InP HBT IC technology for terahertz frequencies: Fundamental oscillators up to 0.57 THz," *IEEE J. Solid-State Circuits* **46**, 2203 (2011).
- ¹²S. Vainshtein and J. Kostamovaara, "Transmission subterahertz imaging utilizing milliwatt-range nanosecond pulses from miniature, collapsing-domain-based avalanche source," in *Terahertz and Mid Infrared Radiation: Detection of Explosives and CBRN (Using Terahertz)*, edited by M. F. Pereira and O. Shulika (Springer, Dordrecht, 2014), Chap. 23, p. 175.
- ¹³S. Vainshtein, V. Yuferev, J. Kostamovaara, M. Kulagina, and H. Moilanen, "Significant effect of emitter area on the efficiency, stability and reliability of picosecond switching in a GaAs bipolar transistor structure," *IEEE Trans. Electron Devices* **57**, 733 (2010).
- ¹⁴T. Grasser, T.-W. Tang, H. Kosina, and S. Selberherr, "A review of hydrodynamic and energy-transport models for semiconductor device simulation," *Proc. IEEE* **91**, 251 (2003).
- ¹⁵D. Vasileska and S. Goodnick, *Computational Electronics* (Morgan & Claypool Publishers, 2006).
- ¹⁶T. Grasser, H. Kosina, C. Heitzinger, and S. Selberherr, "Accurate impact ionization model which accounts for hot and cold carrier populations," *Appl. Phys. Lett.* **80**, 613 (2002).
- ¹⁷R. Stratton, "Diffusion of hot and cold electrons in semiconductor barriers," *Phys. Rev.* **126**, 2002 (1962).
- ¹⁸K. Bløtekjaer, "Transport equations for electrons in two-valley semiconductors," *IEEE Trans. Electron Devices* **17**, 38 (1970).
- ¹⁹S. Selberherr, *Analysis and Simulation of Semiconductor Devices* (Springer, Wien - New York, 1984).
- ²⁰K. Hess, *Advanced Theory of Semiconductor Devices* (Prentice-Hall, Englewood Cliffs, 1988).
- ²¹B. Meinertzhagen and W. L. Engl, "The influence of the thermal equilibrium approximation on the accuracy of classical two-dimensional numerical modeling of silicon submicrometer MOS transistors," *IEEE Trans. Electron Devices* **35**, 689 (1988).
- ²²E. M. Azoff, "Energy transport numerical simulation of graded AlGaAs/GaAs heterojunction bipolar transistors," *IEEE Trans. Electron Devices* **36**, 609 (1989).
- ²³M. Lundstrom, *Fundamentals of Carrier Transport (Modular Series on Solid State Devices)* (Addison-Wesley, Reading, 1990), Vol. 10.
- ²⁴D. K. Ferry, *Semiconductors* (Macmillan, New York, 1991).
- ²⁵Y. Apanovich, E. Lyumkis, B. Polsky, A. Shur, and P. Blakey, "Steady-state and transient analysis of submicron devices using energy balance and simplified hydrodynamic models," *IEEE Trans. Comput. Aided Des.* **13**, 702 (1994).
- ²⁶W. Hänsch, M. Orlowski, and W. Weber, "The hot-electron problem in submicron MOSFET," *J. Phys.* **49**, c4-597 (1988).
- ²⁷W. Hänsch and M. Miura-Mattausch, "The hot-electron problem in small semiconductor devices," *J. Appl. Phys.* **60**, 650 (1986).
- ²⁸S. Vitinov, V. Palankovski, S. Maroldt, and R. Quay, "Physics-based modeling of GaN HEMTs," *IEEE Trans. Electron Devices* **59**, 685 (2012).
- ²⁹R. Redmer, J. R. Madureira, N. Fitzer, S. M. Goodnick, W. Schattke, and E. Schoell, "Field effect on the impact ionization rate in semiconductors," *J. Appl. Phys.* **87**, 781 (2000).
- ³⁰S. P. Platt, C. M. Snowden, and R. E. Miles, "Bipolar Monte Carlo - An improved valence band model for GaAs," in *Proceedings of the Gallium Arsenide Applications Symposium* (Rome, 1990), pp. 258-265.
- ³¹V. Palankovski and R. Quay, *Analysis and Simulation of Heterostructure Devices*, edited by S. Selberherr (Springer, Wien-New York, 2004).
- ³²K. Tomizawa, *Numerical Simulation of Submicron Semiconductor Devices* (Artech House, 1993).